

All-sky assimilation of selected water vapour infrared IASI channels at ECMWF: strategy and initial trials.

Stefano Migliorini^{a,b}, Alan Geer^a, Marco Matricardi^a, Stephen English^a

^aEuropean Centre for Medium-Range Weather Forecasts, Reading, UK

^bNational Centre for Earth Observation, University of Reading, Reading, UK

Motivation and definition of the problem

A more extensive use of available satellite data has been a long-standing goal of operational numerical weather prediction (NWP) centres. One of the current strategies to increase the information yield from satellite instruments is to try to make better use of radiance measurements in channels affected by cloud or precipitation.

This is a very challenging goal, as numerical weather prediction models' forecasts of cloud fields can have significant errors especially in the case of small scale, rapidly varying features over convective regions. Fast radiative transfer models also need to deal with a horizontally non-homogeneous atmosphere and to provide an computationally efficient and accurate treatment of multiple scattering due to cloud particles. Furthermore, the presence of cloud can make the relationship between observations and temperature and humidity profiles significantly nonlinear, to the point that current operational data assimilation system may not be able to make an optimal use of these observations.

Despite these difficulties, recent studies (Prates et al., 2013; Stengel et al., 2013) concerning the assimilation of remote sounding observations in the infrared when clouds are present in the instrument's field of view, confirm the findings of earlier investigations (e.g., Pavelin et al., 2008; McNally 2009) and show that the assimilation of a subset of the sounding channels assimilated above the cloud can reduce the mean analysis errors of the atmospheric temperature and water vapour profiles. There is also evidence of error reduction on cloud condensate variables (Martinet et al. 2012).

These results provide a motivation to carry out a detailed investigation of the informative potential of high-spectral resolution infrared sounders in the presence of cloud, particularly regarding channels that are sensitive to water vapour, which are expected to have a smoother response to cloud. The aim is to determine a set of channels of a given infrared sounder that are most suited to estimate humidity fields in all-sky conditions.

All-sky monitoring experiments with IASI data

The fast radiative transfer model RTTOV v11 was used in this study to simulate the radiances in the infrared as measured by the Infrared Atmospheric Sounding Interferometer (IASI, on board Metop). In particular, radiative effects in the presence of cloud were accounted using the existing "scattering parametrization" configuration of RTTOV (Matricardi, 2005).

The current standard cloud overlap parametrization used by RTTOV consists in subdividing a model's slant column into a sufficient number of sub-columns composed of either cloud-free or overcast layers depending on the value of the cumulative cloud cover using the maximum-random overlap assumption. Initial monitoring experiments showed that such configuration is computationally too expensive for operational implementation and was replaced with just one cloudy column having cloud fraction (constant over the whole atmosphere) equal to its maximum value and with one clear column. A comparison between IASI brightness temperature innovations at 1538.75 cm^{-1} – close to the centre of the water vapour band – from two monitoring experiments using either the single- or the multi-column cloud approach shows that the single-column scheme leads in this case to a relatively moderate increase of the existing innovation bias in the tropics (see Figures 1 and 2). More significant differences are expected, however, when considering water vapour sensitive channels with lower peaking jacobians.

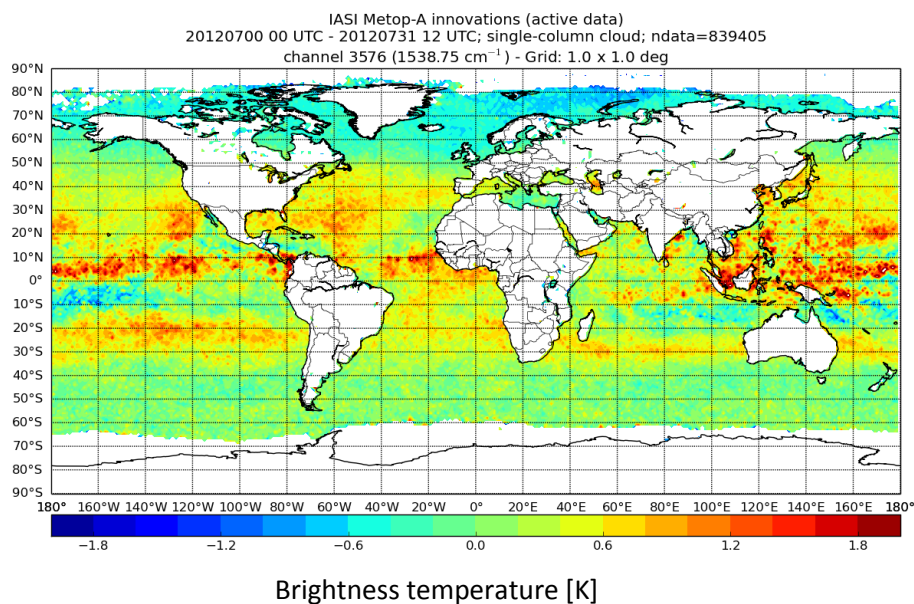


Figure 1 Monthly-mean innovation for IASI channel 3576 (1538.75 cm^{-1}) at 1×1 deg resolution when cloud radiative effects are simulated using the single-column cloud model.

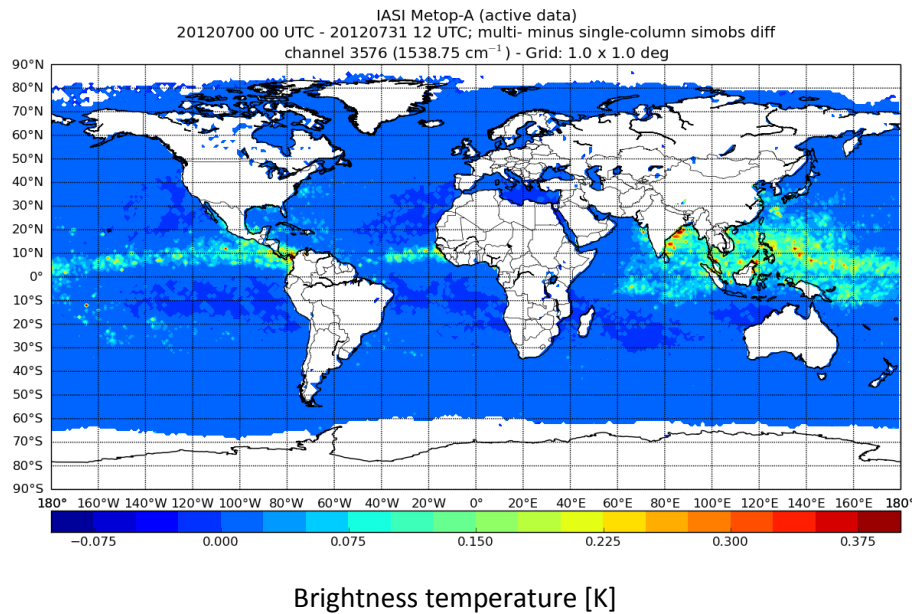


Figure 2 Monthly-mean difference between predicted radiance at IASI channel 3576 (1538.75 cm⁻¹) when using the multi-column cloud model and that when using the single-column model, at 1 × 1 deg resolution.

All-sky IASI data assimilation experiments

The interface to RTTOV 11 used operationally at ECMWF was modified so as to allow the simulation of the radiances from selected IASI channels in all-sky conditions, while other channels are assimilated only in clear-sky.

In the presence of cloud the jacobian of the IASI observation operator is expected to depend critically on the linearization state. Also, temperature and water vapour forecast error uncertainty will be sensitive to the vertical distribution of cloud constituents. For these reasons, forecast sensitivity to all-sky assimilation of IASI data is expected to be flow-dependent and to vary according to the considered set of channels.

Our first experiment consisted in assimilating in all-sky conditions the ten humidity-sensitive IASI channels that are currently assimilated only in clear sky (channel numbers 2889, 2958, 2993, 3002, 3049, 3105, 3110, 5381, 5399 and 5480). In this test the standard observation error in clear sky for these channels (with magnitude 2 K) was replaced with a much larger value – 10 K, in accordance with the value estimated by Okamoto et al.(2013) –, no cloud screening and very loose quality control checks while these ten channels were assimilated in all-sky conditions. A month-long initial assimilation experiment, however, showed that a cloud-independent error model and a selection of channels for assimilation only optimal in clear sky are not sufficient to ensure that an all-sky assimilation of the considered IASI data can result in a better forecast skill than an assimilation of the same channels only in clear sky (see Figure 3).

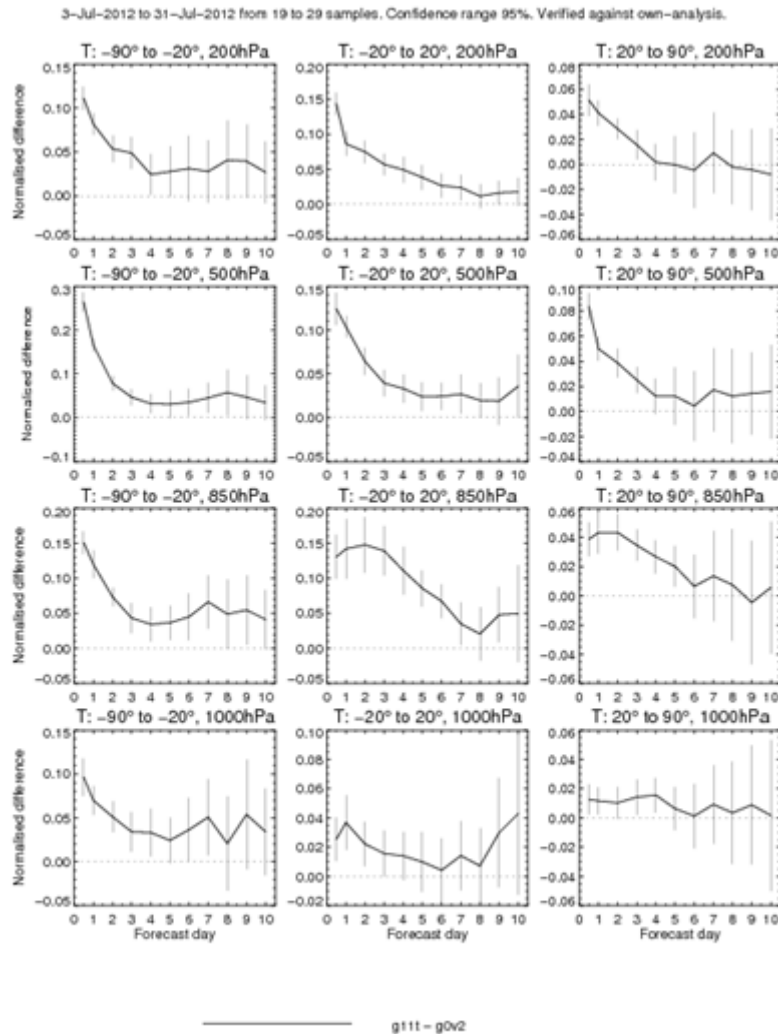


Figure 3 Normalized root-mean-square temperature forecast error difference between experiment with 10 all-sky IASI water vapour channels and experiment with same channels only assimilated in clear sky.

Flow-dependent channel selection in all-sky conditions

The iterative channel selection methodology developed by Rodgers (1996) and used to determine the current set of IASI channels that are assimilated in clear sky (Collard, 2007) was revisited and modified to be used in a consistent way with observations having correlated errors and was applied to IASI simulated observations both in clear sky and overcast conditions using flow-dependent forecast errors as estimated from 50 “ensemble of data assimilations” (EDA) ECMWF forecast members over 91 model levels for a case study during summer 2012.

The iterative channel selection method used here avoids the use of the sequential retrieval error covariance update formula and can then consistently be used in the presence of correlated observation errors. The increased computational cost incurred when avoiding the sequential update proved to be affordable without using high-performance computing resources, also considering that the method is not supposed to be used for near-real-time applications. As in Rodgers (1996), the figure of merit used to select the channels is still

given by the number of degrees of freedom for signal (DFS), but the DFS are now calculated from the signal-to-noise matrix, as discussed below.

At the first iteration step $l=1$ the instrument channel i is considered and the signal-to-noise matrix $\mathbf{S}_{l=1,i} \in \mathbb{R}^{1 \times n}$ is calculated as

$$\mathbf{S}_{l=1,i} = \frac{\mathbf{h}_i^T}{\sigma_i^o} \mathbf{X}$$

where \mathbf{h}_i^T and σ_i^o are the row of the observation operator \mathbf{H} and the observation error standard deviation corresponding to the measurement channel i , respectively, while \mathbf{X} is the symmetric square-root of the vertical forecast error covariance at observation location. Then the Gramian $g_{l=1,i} \in \mathbb{R}$ given by $g_{l=1,i} = \mathbf{S}_{l=1,i} \mathbf{S}_{l=1,i}^T \equiv \lambda_{l=1,j=1,i}^2$ is computed, where the index j orders the singular values of $\mathbf{S}_{l=1,i}$. Then the number $d_{s_{l=1,i}}$ of DFS for channel i is calculated as

$$d_{s_{l=1,i}} = \frac{\lambda_{l=1,j=1,i}^2}{1 + \lambda_{l=1,j=1,i}^2}$$

At iteration step $l=1$ the Gramian $g_{l=1,i}$ and the number of DFS $d_{s_{l=1,i}}$ are calculated m times – where $m=8461$ is the number of IASI channels –, with $i=1, \dots, m$. It is important to note that these computations can be performed in parallel. The channel selected at $l=1$ is the channel i_1 with $d_{s_{l=1,i_1}} = \max(d_{s_{l=1,i}})$, with $i=1, \dots, m$.

The iteration step $l=2$ consists in calculating $\mathbf{S}_{l=2,i} \in \mathbb{R}^{2 \times n}$ as

$$\mathbf{S}_{l=2,i} = \mathbf{R}_{l=2,i}^{-1/2} \begin{pmatrix} \mathbf{h}_{i_1}^T \\ \mathbf{h}_i^T \end{pmatrix} \mathbf{X}$$

where $\mathbf{R}_{l=2,i} \in \mathbb{R}^{2 \times 2}$ is a submatrix of the observation error covariance \mathbf{R} involving its elements i and i_1 . The Gramian matrix $\mathbf{G}_{l=2,i} \in \mathbb{R}^{2 \times 2}$, with $i \neq i_1$, is then given by $\mathbf{G}_{l=2,i} = \mathbf{S}_{l=2,i} \mathbf{S}_{l=2,i}^T \equiv \mathbf{U}_{l=2,i} \mathbf{\Lambda}_{l=2,i}^2 \mathbf{U}_{l=2,i}^T$, where $\mathbf{U}_{l=2,i}$ and $\mathbf{\Lambda}_{l=2,i}^2$ are the matrices of the eigenvectors and of the eigenvalues of $\mathbf{G}_{l=2,i}$. Then the number of DFS for channel $i \neq i_1$ is calculated as

$$d_{s_{l=2,i}} = \sum_{j=1}^r \frac{\lambda_{l=2,j=1,i}^2}{1 + \lambda_{l=2,j=1,i}^2}$$

with $r \leq \min(2, n)$. At iteration step $l=2$ the Gramian matrix $\mathbf{G}_{l=2,i}$ and the number of DFS $d_{s_{l=2,i}}$ are calculated $m-1$ times, with $i=1, \dots, m \neq i_1$. The channel selected at $l=2$ is the channel i_2 with $d_{s_{l=2,i_2}} = \max(d_{s_{l=2,i}})$, with $i=1, \dots, m \neq i_1$. The algorithm is iterated until $l=n_{\text{sel}}$ channels are selected.

The number of DFS achieved by the selected channels (100 for temperature and additional 50 including water vapour contributions) for our case study for the 135 almost surely clear-sky locations – abbreviated as a.s. and defined as the location where all EDA members are cloud free – and the 169 a.s. overcast locations are shown in Figure 4.

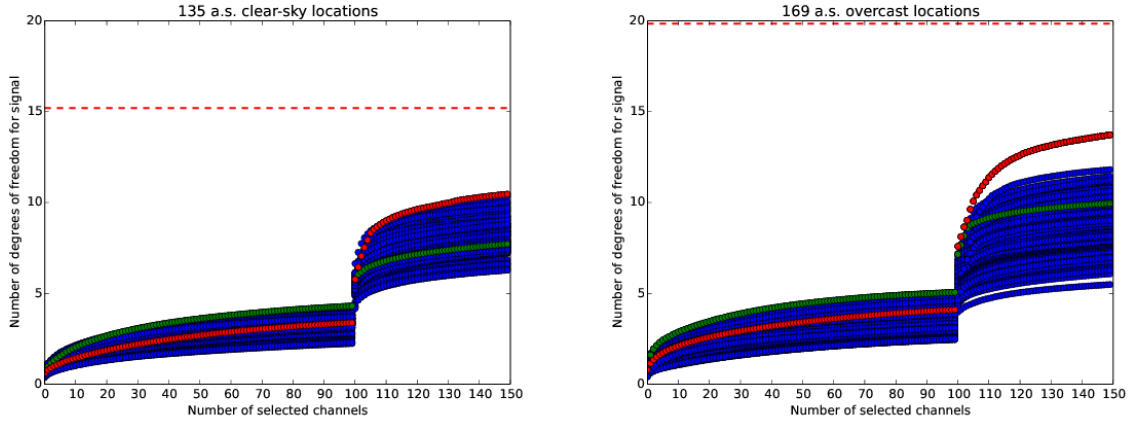


Figure 4 Number of degrees of freedom for signal (DFS) achieved in a.s. clear-sky (left panel) and in a.s. overcast (right panel) conditions when selecting first up to 100 temperature-sensitive IASI channels and then when selecting up to additional 50 channels that are sensitive to water vapour. The red dashed line represents the number of DFS obtained when all 8461 IASI channels are considered, at the a.s. clear-sky and a.s. overcast locations where the largest values of DFS are achieved for the maximum number of selected channels. The number of DFS for the channels selected at these locations are denoted by red dots, while the number of DFS for the channels selected at the locations where the largest values of DFS are achieved for the maximum number of selected temperature channels are denoted by green dots.

At each a.s. overcast or a.s. clear-sky location are selected 50, generally different, humidity sensitive channels. The final shortlist is determined by the channels that are selected at least at 40% of both a.s. overcast and a.s. clear-sky locations. A final ranking q_i of the shortlisted (in this case 22) channels (see Figure 5, 6 and Table 1) can be obtained by calculating the average between the all-sky-average selection frequency f_i and the all-sky-average relative ranking order p_i defined as $p_i = 100 \times \frac{n_{sel} - n_i}{n_{sel} - 1}$ where n_{sel} is the number of selected channels (in this case 50) and n_i is the ranking order of channel i . For example, $n_i = 1$ means that channel i provides the largest increase in DFS on humidity given the previously selected – in this case 100 – temperature sensitive channels and then $p_i = 100\%$.

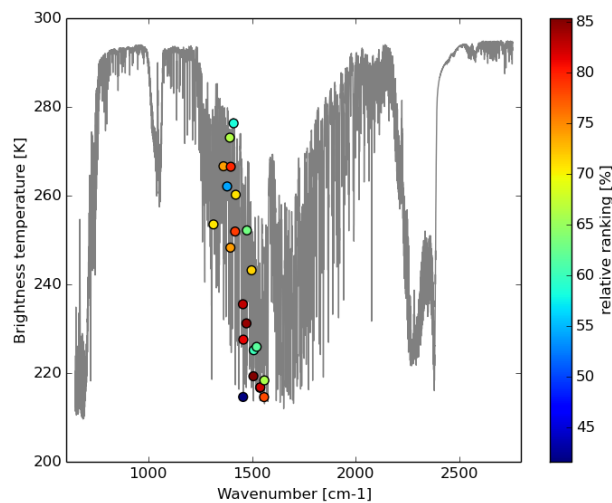


Figure 5 Spectral locations (indicated by coloured circles) of a set of 22 humidity-sensitive IASI channels as selected using the iterative, non-sequential channel selection procedure described in this work. The colour scale denotes the ranking value q_i taken by each selected channel (see text).

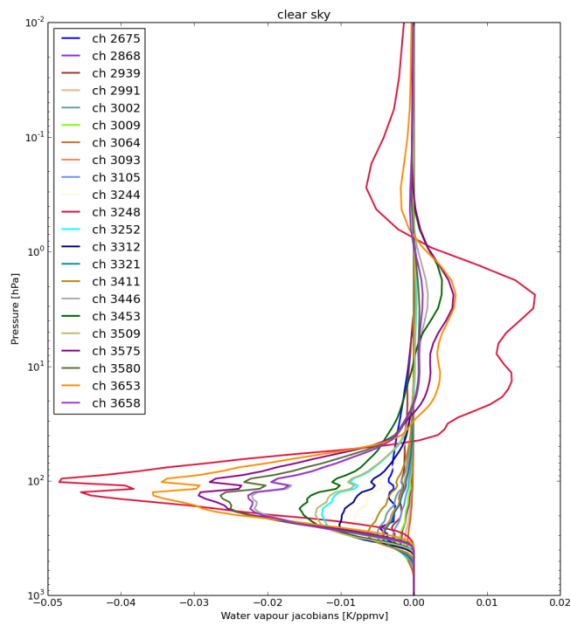


Figure 6 Humidity jacobians of the 22 selected channels

IASI channel number	wavenumber (cm ⁻¹)	channel ranking (%)	ranking order
2675	1313.5	70.77	13
2868	1361.75	73.92	10
2939	1379.5	54.18	21
2991	1392.5	66.22	14
3002	1395.25	74.24	9
3009	1397	79.69	6
3064	1410.75	58.45	19
3093	1418	78.66	7
3105	1421	70.83	12
3244	1455.75	82.85	3
3248	1456.75	41.60	22
3252	1457.75	81.32	5
3312	1472.75	84.40	2
3321	1475	62.99	16
3411	1497.5	71.63	11
3446	1506.25	85.34	1
3453	1508	60.07	18
3509	1522	61.72	17
3575	1538.5	54.98	20
3580	1539.75	82.28	4
3653	1558	77.96	8
3658	1559.25	66.03	15

Table 1 Humidity-sensitive IASI channels selected using the procedure described in the text. The IASI channel numbers in the left column shown in italic or in bold are currently operationally monitored or assimilated, respectively. See text for a definition of channel ranking.

Summary and future work

In this study a set of 100 temperature-sensitive and 50 humidity-sensitive IASI channels below 2200 cm^{-1} (to avoid solar contamination) were selected at a number of clear-sky and overcast locations for a case study in July 2012. Care was taken to select a final short-list of 22 humidity-sensitive channels according to flow-dependent estimates of the forecast error uncertainty of the NWP model in all-sky conditions. To this end, a novel channel selection method that is non-sequential and capable of accounting for observation error correlation was developed. Finally, new capability to simulate IASI channels either in clear-sky or when emerging radiation is affected by cloud was introduced in the interface to RTTOV v11 used operationally at ECMWF.

The forecast impact of the all-sky v. clear-sky assimilation of the selected humidity-sensitive channels is being assessed by means of a set of twin experiments. Preliminary tests, however, indicate that to achieve a positive outcome it is essential to ensure the following: a) use of suitable channel selection procedures; b) observation error uncertainty levels and quality control strategies used for data assimilation should depend on the presence of cloud in the instrument field of view and/or in the model prediction of the observation.

Acknowledgements

The authors would like to thank F. Baordo, M. Bonavita, N. Bormann, R. Eresmaa, M. Hamrud, E. Holm, C. Lupu and T. McNally for their useful comments.

References

- P. Martinet, N. Fourrié, V. Guidard, F. Rabier, T. Montmerle and P. Brunel. "Towards the use of microphysical variables for the assimilation of cloud-affected infrared radiances". *Q. J. R. Meteorol. Soc.*, 2012, doi: 10.1002/qj.2046
- M. Matricardi. "The inclusion of aerosols and clouds in RTIASI, the ECMWF fast radiative transfer model for the infrared atmospheric sounding interferometer". *ECMWF Tech. Memo.*, 474, 2005.
- A. P. McNally. "The direct assimilation of cloud-affected satellite infrared radiances in the ECMWF 4D-Var". *Q. J. R. Meteorol. Soc.*, 135: 1214–1229, 2009. doi: 10.1002/qj.426
- Okamoto, K., McNally, A. P. and Bell, W. "Progress towards the assimilation of all-sky infrared radiances: an evaluation of cloud effects". *Q.J.R. Meteorol. Soc.*. 2013, doi: 10.1002/qj.2242
- E. G. Pavelin, S. J. English and J. R. Eyre, "The assimilation of cloud-affected infrared satellite radiances for numerical weather prediction". *Q. J. R. Meteorol. Soc.*, 134: 737–749, 2008. doi: 10.1002/qj.243
- C. Prates, S. Migliorini, S. English and Ed Pavelin. "Assimilation of satellite infrared sounding measurements in the presence of clouds," *Q. J. R. Meteorol. Soc.*, 2013, doi: 10.1002/qj.2279

C.D. Rodgers. "Information content and optimization of high-spectral-resolution measurements", SPIE's 1996 International Symposium on Optical Science, Engineering, and Instrumentation, 1996, pp 136--147.

M. Stengel, M. Lindskog, P. Undén and N. Gustafsson. "The impact of cloud-affected IR radiances on forecast accuracy of a limited-area NWP model," *Q. J. R. Meteorol. Soc.*, 2013, doi:10.1002/qj.2012.